# Chaotic-Cavity Surface-Emitting Lasers for Optical Wireless Communication

**Omar Alkhazragi[1], Ming Dong[1], Liang Chen[1], Dong Liang[2], Tien Khee Ng[1], Junping Zhang[2,3], Hakan Bagci[1,4], and Boon S. Ooi[1,5]**

*[1]Division of Computer, Electrical, and Mathematical Science and Engineering, King Abdullah University of Science and Technology (KAUST), Thuwal 23955-6900, Saudi Arabia*

*[2]Huawei Technologies Co., Ltd., Shenzhen 518129, China*

*e-mail addresses: [3]junping.zhang@huawei.com, [4]hakan.bagci@kaust.edu.sa, [5]boon.ooi@kaust.edu.sa*

**Abstract:** We demonstrated using chaotic cavities to lower the spatial coherence of vertical-cavity surface-emitting lasers. Our design achieved a 10-Gb/s data rate with a 60% increase in the optical power and double the number of modes. 

## 1. Introduction

The high coherence of lasers can be beneficial in a variety of applications. However, it introduces limitations due to the formation of coherence artefacts (speckles) caused by random scattering of photons along the propagation path. This results in poor performance in imaging, illumination, and display applications. In addition, the relatively long coherence length limits the resolution in interference-based sensing, including optical coherence tomography (OCT) and fiber-optic gyroscopes (OCT). These shortcomings have given rise to the development of low-coherence semiconductor light sources, such as low-coherence edge-emitting lasers [1], superluminescent diodes (SLDs) [2], and random lasers [3]. However, to date, the operation of all these devices relies on horizontal waveguides with edge-emitting configurations. Therefore, they lack the intrinsic unique advantages of vertical-cavity surface-emitting lasers (VCSELs), which hinders their utilization in a variety of applications.

The recent adoption of VCSELs in consumer electronics resulted in a new surge of interest in their capabilities. The ease of manufacturing 2D arrays of VCSELs makes them the semiconductor laser of choice in many applications in sensing (e.g., light detection and ranging (LiDAR)) and high-speed communication (e.g., indoor wireless attocell networks) [4]. Furthermore, recent advances in the development of GaN-based visible-light VCSELs are expected to enable even more applications in the near future. Nevertheless, all high-speed VCSELs still suffer from issues caused by the high coherence of the light they emit. To circumvent this bottleneck, we report on the use of chaotic-cavity designs to increase the number of transverse modes emitted from VCSELs without increasing their size. The adopted D-shaped chaotic cavity is shown to result in an increase in the achievable optical power of up to 60% while doubling the number of transverse modes which yields a lower spatial coherence. Moreover, the difference in the wavelength of the different modes results in an increase in the full width at half maximum (FWHM) of the emission linewidth from around 1.0 nm to 4.6 nm, which indicates a significant reduction in the temporal coherence of the emitted light. Finally, we used the chaotic-cavity VCSEL as the transmitter in an optical wireless communication (OWC) link. The modulation bandwidth of the chaotic-cavity VCSEL is around 4 GHz, which is significantly higher than other low-coherence light sources, such as light-emitting diodes (LEDs) and SLDs. Using this new class of VCSELs with orthogonal frequency-division multiplexing (OFDM), which makes use of the higher efficiency of chaotic-cavity VCSELs for more efficient data loading, the achieved net data rate is 10 Gb/s. This demonstration paves the way toward the development of low-coherence surface-emitting lasers (LCSELs), which combine the advantages of low-coherence sources with the surface-emission of VCSELs to enable a wide range of applications ranging from imaging, to sensing, to simultaneous illumination and high-speed communication using visible-light VCSELs.

## 2. Results and Discussion

To demonstrate the effects of using chaotic cavities in VCSEL design, we fabricated two types of broad-area VCSELs with similar emission areas on the same 940-nm VCSEL wafer: (1) a conventional VCSEL with a circular mesa (O-shaped henceforth) and (2) a chaotic-cavity VCSEL with a D-shaped mesa. Figure 1(a) shows a scanning electron microscope (SEM) image of two adjacent VCSELs having the two tested cavity designs. Over the 189 VCSELs tested (102 are D-shaped), the D-shaped VCSELs, on average, achieves 67% higher optical power. Figure 1(b) shows the light output versus current (L–I) plots of a representative pair of VCSELs. The increase in the optical power is due to the more uniform distribution of the optical field inside the cavity. This is clearly shown by the near-field profiles of the O- and D-shaped VCSELs provided in Figs. 1(c) and 1(d), respectively.

To verify the increase in the number of transverse modes, we have measured the spectra of two adjacent VCSELs [as shown in Fig. 1(a)]. Figure 1(e) shows the spectra around the maximum optical power of each device. It is observed that the D-shaped VCSEL exhibits a wider spectral emission with a FWHM around 4.6 nm compared to 1.0 nm from the O-shaped VCSEL. The FWHM values at different injection currents of representative VCSELs are shown in Fig.

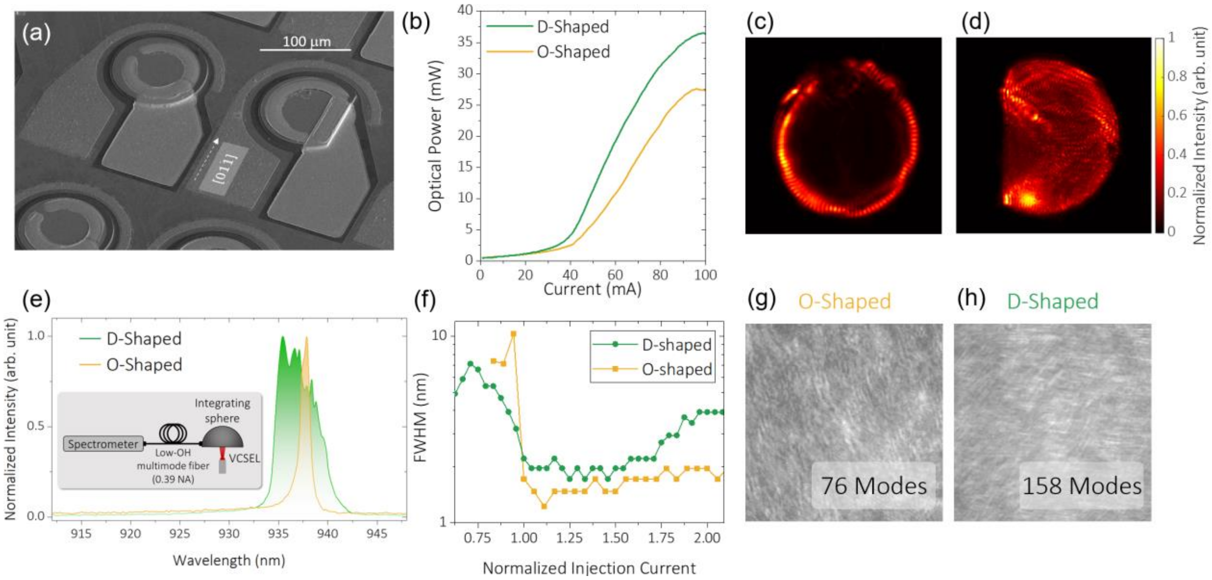


Figure 1. (a) Scanning electron microscope (SEM) image of adjacent VCSELs. (b) L–I plots of two VCSELs with different mesa shapes. Pictures in (c) and (d) are near-field images of an O-shaped and a D-shaped VCSEL, respectively. The images are captured at similar optical powers (10 mW). (e) Spectra of the two VCSEL shapes around their respective maximum powers. The inset shows the measurement setup. (f) Full width at half maximum (FWHM) values at different injection currents (normalized by the respective thresholds) for two representative VCSELs. (g) and (h) are the speckle patterns from the O- and D-shaped VCSELs around their maximum optical power.

1(f). A substantial increase in the FWHM is observed only for the D-shaped VCSEL. This is due to the increased number of modes supported by the cavity. However, given the limited resolution of the spectrometer, the spectra of individual modes cannot be identified. To confirm the increase in the number of modes, we have recorded the speckle patterns from the two VCSELs around their maximum powers after passing their beams through a diffuser. By calculating the inverse of the square of the speckle contrast (the standard deviation of the intensity after normalizing by the mean) [5], the number of mutually incoherent modes of the O- and D-shaped VCSELs is estimated to be 76 and 158, respectively.

The communication performance using the chaotic-cavity VCSEL was then studied. The higher optical power of the chaotic-cavity VCSEL can help in increasing the data rate in OWC. This is because increasing the power can improve the signal-to-noise ratio (SNR) of the received signal, allowing for more bits to be loaded with higher spectral efficiency modulation schemes. Given that, we used a chaotic-cavity D-shaped VCSEL with a maximum optical power of around 36 mW as the transmitter in an OWC link with DC-biased optical OFDM (DCO-OFDM) and quadrature amplitude modulation (QAM).

We first measured the frequency response of the O- and D-shaped broad-area VCSELs using an InGaAs photodetector (Newport, 818-BB-35A) with a 10-GHz bandwidth as the receiver. A variable optical attenuator is placed in front of the detector to make sure the received signal is within its dynamic range. The normalized frequency response plots recorded using a vector network analyzer (Agilent, E8361C) after calibration using an electronic calibration module (Agilent, 85093-60010) are shown in Figs. 2(a) and 2(b) for the O-and D-shaped VCSELs,

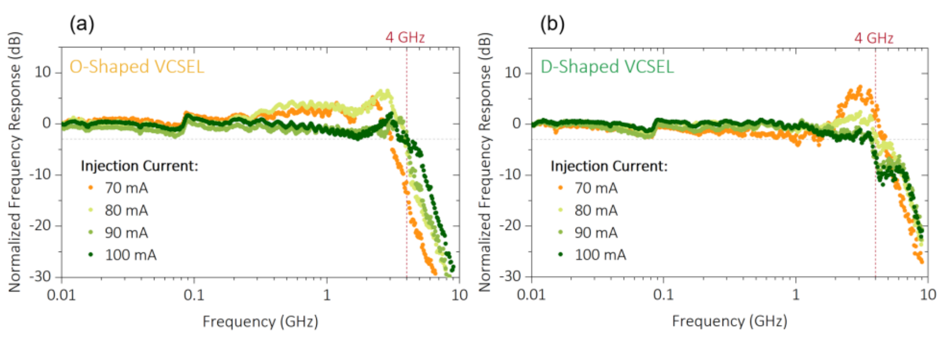


Figure 2. The measured normalized frequency response at different injection current values using (a) the O-shaped and (b) the D-shaped VCSELs as the transmitter.

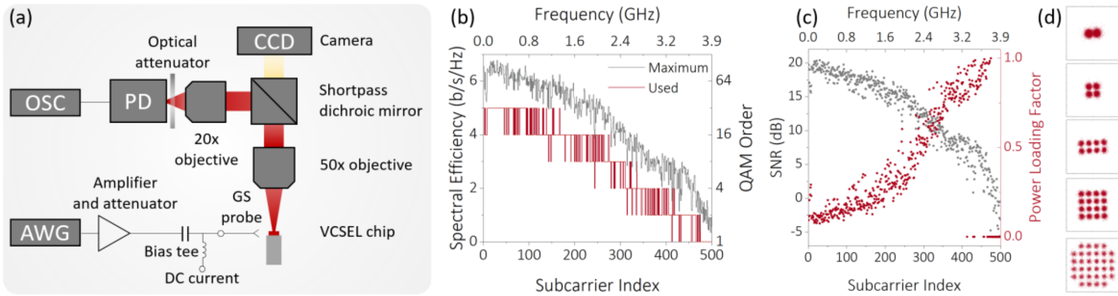


Figure 3. (a) The OWC setup. (b) The maximum and the used spectral efficiency for each subcarrier in the 4-GHz signal. (c) The SNR and the power loading factor for each subcarrier. (d) Constellation diagrams of the received signal. All subcarriers with the same QAM order are combined in the same diagram.

respectively, at different injection current above threshold. It can be seen that the –3-dB modulation bandwidth for both VCSELs is found to be around 4 GHz. This is significantly broader than low-coherence sources such as edge-emitting SLDs (the highest reported bandwidth is around 2.5 GHz with a maximum optical power of 17 mW [6]). Therefore, the chaotic-cavity VCSEL achieves a lower coherence compared to conventional VCSELs without resorting to increasing the VCSEL size, which would substantially limit its modulation bandwidth.

The OFDM signal was then generated to make use of the 4-GHz bandwidth and the high SNR. The communication setup is shown in Fig. 3(a). The sampling rates of the arbitrary waveform generator (AWG, Tektronix, AWG70002A) and the oscilloscope (OSC, Tektronix, DPO 72004C) were set to 8 and 25 GSample/s, respectively. A 4-GHz amplifier (Mini-Circuits, ZHL-42W+) and a variable attenuator are used to control the signal amplitude from the AWG (whose maximum amplitude is limited to 250 mV), which is then combined with the DC bias using a bias-tee. The combined signal is fed to the chaotic-cavity VCSEL through a ground-signal (GS) probe. The size of the fast Fourier transform (FFT) was set to 1,024 and that of the cyclic prefix was set to 10. 500 subcarriers were used starting from the $6^{th}$ subcarrier to avoid the low response in the low frequency band. 150 OFDM symbols were sent with 8 of them used as training symbols for synchronization and post equalization. First, a uniform 4-QAM test signal was sent to measure the SNR for each subcarrier. Then, by calculating the maximum channel capacity for each subcarrier, bit- and power-loading schemes were implemented, as shown in Figs. 3(b) and 3(c). The result of these schemes is a signal with a gross data rate of 11.4 Gb/s with a bit error ratio of $3.7\times10^{-3}$ [Fig. 3(d) shows the constellation diagrams of the received signal], which is below the 7%-overhead forward error correction (FEC) limit of $3.8\times10^{-3}$. After accounting for the 5.3% training symbols and the 7% overhead required for FEC, the net data rate is 10.0 Gb/s, which is more than double the record data rate achieved using SLDs (4.6 Gb/s) [7].

## 3. Conclusions

We demonstrate for the first time the use of chaotic cavity to lower the coherence of VCSELs. We show that using a D-shaped chaotic cavity doubles the number of transverse modes and increases the achievable optical power due to a more uniform distribution of the optical field. The proposed design does not require any additional cost, footprint, nor fabrication steps, which allows for using this new class of VCSELs in a wide range of applications ranging from wireless communication to sensing to speckle-free imaging. The performance of the chaotic-cavity VCSEL in an OWC link is demonstrated and a net data rate of 10 Gb/s is achieved, which is more than double the SLD record.

## Acknowledgement

The authors acknowledge funding support from Huawei Technologies Co., Ltd. (YBN2020085017).

## References

[1] B. Redding *et al.*, "Low spatial coherence electrically pumped semiconductor laser for speckle-free full-field imaging," *Proc. Natl. Acad. Sci. USA*, vol. 112, no. 5, pp. 1304–1309, 2015.
[2] C. Shen *et al.*, "Group-III-Nitride Superluminescent Diodes for Solid-State Lighting and High-Speed Visible Light Communications," *IEEE Journal of Selected Topics in Quantum Electronics*, vol. 25, no. 6, p. 2000110, 2019.
[3] A. Consoli, N. Caselli, and C. López, "Electrically driven random lasing from a modified Fabry–Pérot laser diode," *Nat. Photonics*, vol. 16, no. 3, pp. 219–225, 2022.
[4] E. Sarbazi, H. Kazemi, M. D. Soltani, M. Safari, and H. Haas, "A Tb/s Indoor Optical Wireless Access System Using VCSEL Arrays," in *2020 IEEE 31st Annual International Symposium on Personal, Indoor and Mobile Radio Communications*, 2020, pp. 1–6.
[5] J. W. Goodman, "Optical Methods for Suppressing Speckle," in *Speckle Phenomena in Optics: Theory and Applications, Second Edition*, SPIE, 2020, pp. 175–223.
[6] A. Rashidi *et al.*, "High-Speed Nonpolar InGaN/GaN Superluminescent Diode With 2.5 GHz Modulation Bandwidth," *IEEE Photonics Technology Letters*, vol. 32, no. 7, pp. 383–386, 2020.
[7] D. Li *et al.*, "High-Speed GaN-Based Superluminescent Diode for 4.57 Gbps Visible Light Communication," *Crystals*, vol. 12, no. 2., p. 191 2022.